Molecules and Cells

Lipopolysaccharide (LPS)-Induced Autophagy Is Responsible for Enhanced Osteoclastogenesis

Ok-Joo Sul[1,2], Hyun-Jung Park[1,2], Ho-Jung Son[1], and Hye-Seon Choi[1,*]

[1]Department of Biological Sciences, University of Ulsan, Ulsan 44610, Korea, [2]These authors contributed equally to this work.
*Correspondence: hschoi@mail.ulsan.ac.kr
http://dx.doi.org/10.14348/molcells.2017.0230
www.molcells.org

We hypothesized that inflammation affects number and activity of osteoclasts (OCs) via enhancing autophagy. Lipopolysaccharide (LPS) induced autophagy, osteoclastogenesis, and cytoplasmic reactive oxygen species (ROS) in bone marrow-derived macrophages that were pre-stimulated with receptor activator of nuclear factor-κB ligand. An autophagy inhibitor, 3-methyladenine (3-MA) decreased LPS-induced OC formation and bone resorption, indicating that autophagy is responsible for increasing number and activity of OCs upon LPS stimulus. Knockdown of autophagy-related protein 7 attenuated the effect of LPS on OC-specific genes, supporting a role of LPS as an autophagy inducer in OC. Removal of ROS decreased LPS-induced OC formation as well as autophagy. However, 3-MA did not affect LPS-induced ROS levels, suggesting that ROS act upstream of phosphatidylinositol-4,5-bisphosphate 3-kinase in LPS-induced autophagy. Our results suggest the possible use of autophagy inhibitors targeting OCs to reduce inflammatory bone loss.

Keywords: autophagy, lipopolysaccharide, osteoclast

INTRODUCTION

Lipopolysaccharide (LPS) is an important component of the cell wall of Gram-negative bacteria. Injection of LPS increases the area of eroded surface in rat femurs along with a significant elevation of the number of osteoclasts (OC) (Orcel et al., 1993), whereas *in vitro* the effect of LPS has been demonstrated to be of two kinds with respect to receptor activator of nuclear factor-κB ligand (RANKL)-mediated OC formation. Osteoclastogenesis was enhanced in pre-OCs only when they were treated with RANKL before being exposed to LPS (Park et al., 2014) whereas it was inhibited when LPS and RANKL were added simultaneously (Takami et al., 2002), suggesting that LPS plays a role in enhancing OC formation, but is not effective in early progenitors of OCs.

Autophagy is characterized by phagophore formation and subsequent fusion of autophagosome with lysosomes, and was initially discovered as a cell survival mechanism in response to nutrient starvation. However, unnecessary or dysfunctional cellular components are degraded and removed by autophagy under physiological conditions, suggesting that autophagy acts to preserve the balance between organelle biogenesis and protein synthesis, and their breakdown. Dysregulated autophagy has been implicated in the development of several diseases. Pathway analysis based on human genome-wide association data showed that regulation of autophagy was associated with the development of osteoporosis (Zhang et al., 2010), indicating a close link between autophagy and bone metabolism. This association is supported by the bone-sparing effects of PI3K inhibitors, wortmannin and LY301497 that all prevented ovariectomy (OVX)-induced bone loss *in vivo* and lowered the bone resorbing activity of OCs *in vitro* (Sato et al., 1996). Defective microtubule-dependent podosome belt formation in OCs has been reported in response to nocodazole, an inhibitor of PI3K (Ti et al., 2015), showing that inhibition of autophagy affects the activity of OCs. In addition Lin et al. (2013) have demonstrated that beclin1 and Atg7, which are involved

Received 25 September, 2017; revised 12 October, 2017; accepted 16 October, 2017; published online 16 November, 2017

eISSN: 0219-1032

in the initiation and elongation of phagophores during autophagy, increase in the OCs of rheumatoid arthritis patients, suggesting that increased autophagy in OCs leads to bone destruction *in vivo*. However, inhibition of mTOR by sirolimus or everolimus reduced OC formation and protected against local bone erosion in experimental arthritis (Cejka et al., 2010), implying an opposite effect of autophagy on bone. Over-expression of tumor necrosis factor (TNF) using TNF-transgenic mice resulted in elevated levels of Atg7 and beclin 1 in OCs (Cejka et al., 2010), supporting the view that inflammation leads to enhanced autophagy in OCs.

In the present study we have investigated whether autophagy plays a role in LPS-stimulated osteoclastogenesis *in vitro*.

MATERIALS AND METHODS

Animals and OC formation

All mice were handled in accordance with the guidelines of the Institutional Animal Care and Use Committee (IACUC) of the Immunomodulation Research Center (IRC), University of Ulsan. All animal procedures were approved by the IACUC of the IRC. The approval ID for this study is # UOU-2014-010. Bone marrow cells were isolated from 4-5-week-old C57BL/6J mice as described before (Ke et al., 2014). Femora and tibiae were removed aseptically and dissected free of adherent soft tissue. The bone ends were cut, and the marrow cavity was flushed out with α-MEM from one end of the bone using a sterile 21-gauge needle, and agitation with a Pasteur pipette was used to get a single cell suspension. The resulting bone marrow suspension was washed twice, and incubated on plates along with M-CSF (20 ng/ml) (R&D Systems, USA) for 16 h. Non-adherent cells were harvested, layered on a Ficoll-hypaque gradient for collecting the cells at the interface, and cultured for two more days, at which time large populations of adherent monocyte/macrophage-like cells had formed on the bottom of the culture plates, as described before (Ke et al., 2014). The small numbers of non-adherent cells were removed by washing the dishes with phosphate-buffered saline (PBS), and the remaining, adherent, cells (bone marrow-derived macrophages (BMM)) were harvested, and seeded in plates. The adherent cells were analyzed with a FACSCalibur flow cytometer (Becton Dickinson, USA) and found to be negative for CD3 and CD45R, and positive for CD11b. The absence of contaminating stromal cells was confirmed by lack of growth without addition of M-CSF. Pre-OC cells were generated by incubation with M-CSF and RANKL (R&D Systems) for 40 h, and these cells were treated with M-CSF and LPS (Sigma Chemical., USA) for 48 h to generate OCs. A sample of these cells was fixed in 10% formalin for 10 min, and stained for tartrate-resistant acid phosphatase (TRAP) as described (Ke et al., 2014). Numbers of TRAP-positive multinucleated cells (MNC) (three or more nuclei) were scored.

Bone resorption *in vitro*

OCs were further characterized by assessing their ability to form pits on dentine slices (Jimi et al., 1999). Mature OC were seeded on dentine slices (Immunodiagnostic Systems, UK) and incubated for 3 days with M-CSF and LPS in the presence or absence of 3-MA. The slices were cleaned by ultrasonication in 1 M NH_4OH to remove adherent cells and stained with Mayer's hematoxylin (Sigma) to visualize resorption pits. Resportion pit areas were measured with Image J 1.37v.

RNA isolation and quantitative polymerase chain reaction (qPCR)

Total RNA was reverse-transcribed with random primers and M-MLV reverse transcriptase (Promega, USA). qPCR was carried out using SYBR Green 1 Taq polymerase (Qiagen, Germany) and appropriate primers on a StepOnePlus™ Real Time System (Applied Biosystems, USA). The specificity of each primer pair was confirmed by melting curve analysis and agarose-gel electrophoresis. The housekeeping 18S rRNA (RPS) gene was amplified in parallel with the genes of interest. Relative copy numbers compared to RPS were calculated using $2^{-\Delta\Delta Ct}$. The primer sequences used were as follows: 5'-ttcagttgctatccaggactcgga-3' and 5'-gcatgtcatgtag gtgagaaatgtgctca-3' (ATP6v0d2); 5'-gggccaggatgaaagttgta-3' and 5'-cactgctctcttcagggctt-3' (Cathepsin K); 5'-agttgccctc ttatgaaggagaag-3' and 5'-ggagtgtcgtcccagcacat-3' (calcitonin receptor); 5'-tcctccatgaacaaacagttccaa-3' and 5'-agacgtgg tttaggaatgcagctc-3' (DC-STAMP); 5' gaccaccttggcaatgtctctg-3' 5'-tggctgaggaagtcatctgagttg-3' (TRAP); 5'-atcagagagttga ccgcagttg-3' and 5'-aatgaaccgaagcacaccatag-3' (RPS).

Western bot analysis

Cultured cells were harvested after washing with ice-cold PBS and lysed in extraction buffer (50 mM Trsi-HCl, pH 8.0, 150 mM NaCl, 1 mM EDTA, 0.5% Nonidet P-40, 0.01% protease inhibitor mixture). Cell extracts were subjected to SDS-PAGE and transferred onto nitrocellulose. Membranes were blocked for 1 h with skim milk in Tris-buffered saline containing 0.1% Tween 20 and incubated overnight at 4℃ with Abs against LC3B (#2775, Cell signaling), and β-actin (Santa Cruz Biotechnology). Membranes were washed, incubated for 1 h with HRP-conjugated secondary Abs (Santa Cruz Biotechnology), and developed using chemiluminescence substrates.

Flow-cytometric quantification of AVOs by AO staining

To characterize autophagy, acidic vesicular organelles (AVOs; autophagosomes and autolysosomes) were quantified by flow cytometry after staining with acridine orange (AO) as described (Chen et al., 2007). AO is a fluorescent weak base that accumulates in acidic spaces and fluoresces bright red. In AO-treated cells, the cytoplasm and nucleolus fluoresce bright green and dim red, respectively, whereas AVOs fluoresce bright red. The intensity of the red fluorescence is proportional to the degree of acidity. Cells were stained with a final concentration of 1 μg/ml AO for 20 min. The cells were washed twice with PBS, removed from the plate with trypsin-EDTA and collected. Green (510-530 nm) and red (>650 nm) fluorescence emissions from 1×10^4 cells, illuminated with blue (488 nm) excitation light, were measured using a BD Bioscience FACSCanto II system and FACSDiva software.

Intracellular reactive oxygen species (ROS)

The intracellular formation of ROS was detected using the fluorescent probe, 2',7'-dichlorofluorescein diacetate (H_2DCFDA) (Molecular Probes). BMMs were prepared and incubated with M-CSF and RANKL for 40 h, washed thoroughly, and incubated further for the indicated periods with LPS in the presence of M-CSF, harvested, suspended in PBS, loaded with H_2DCFDA, and incubated at 37℃ for 30 min. Intracellular ROS were measured by flow cytometry.

Transfection of siRNA

BMMs were incubated with M-CSF and RANKL for 40h and transfected with small interfering RNA (siRNA) against NOX1 (sc-43940), NOX2 (sc-14920), and ATG7 (sc-41448) or with scrambled siRNA (scRNA, sc-37007) (Santa Cruz Biotechnology) using lipofectamine 3000 (Invitrogen, USA). In brief, 2.5 μl of siRNA (50 μM) or an equal amount of scRNA was mixed with 3.75 μl of lipofectamine 3000 reagent in a 50 μl Opti-MEM (Gibco, USA) culture medium. After incubation for 15 min, the mixtures were added to 2 × 10^5 cells already plated in 24 well plates. After transfection, the cells were incubated further for the indicated periods with LPS and M-CSF.

Statistical analysis

Values are expressed as means ± SEM. Pairs of groups were compared by Student's *t*-tests, and multiple groups by one-way ANOVA, followed by Bonferroni post-tests. *P* values < 0.05 were considered statistically significant.

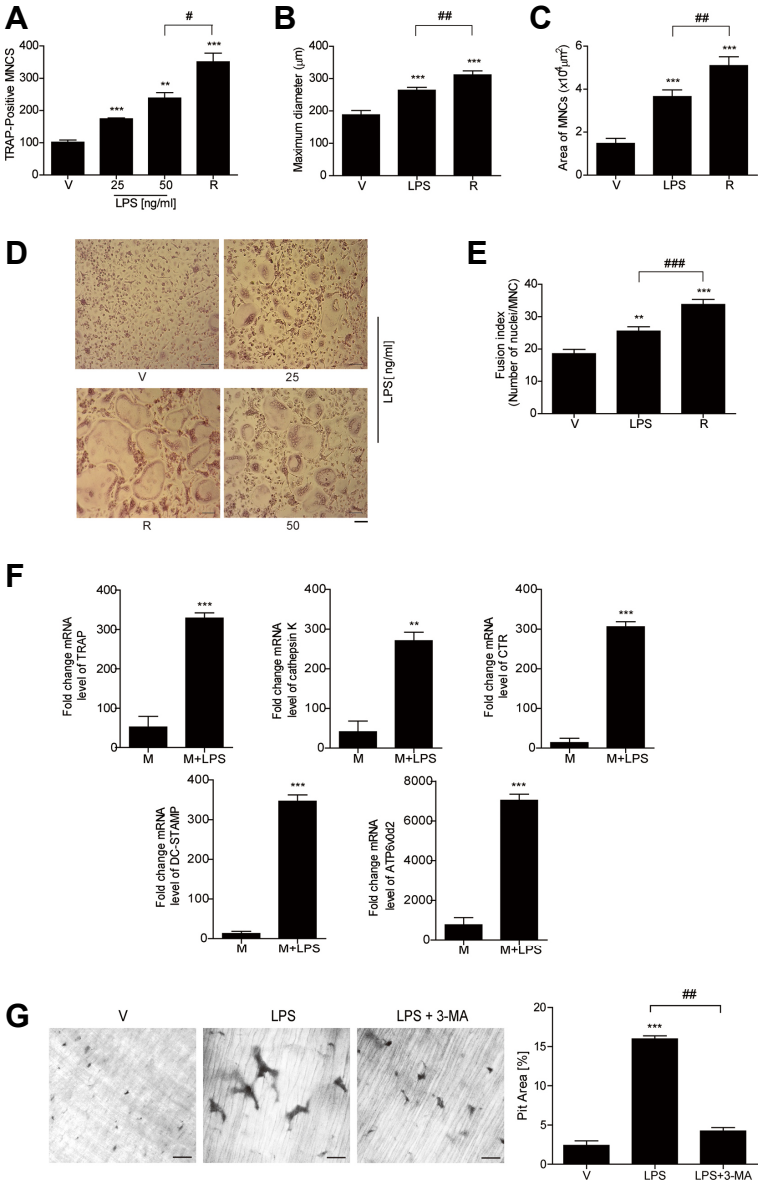

Fig. 1. LPS increases the number and activity of OCs *in vitro*. (A-E) BMMs were prepared and incubated with M-CSF (M, 30 ng/ml) and RANKL (R, 40 ng/ml) for 40 h, washed thoroughly, and incubated further for 48 h with LPS at the indicated concentration or RANKL in the presence of M-CSF. Cells were fixed and TRAP-positive MNCs per well were counted (A). Thereafter, more than 70 TRAP-positive MNCs in each culture were randomly selected, and the maximum diameter (B) and the area (C) of the formed OCs were measured. (D) Representative photos of A. Scale bar; 200 μm. The fusion index was presented as the average number of nuclei per OCs formed in the cultures, which indicted the number of cells that participates in fusion (E). (F) RNA from pre-OC cells which were treated with M-CSF and RANKL for 40 h, and stimulated with LPS (50 ng/ml) in the presence of M-CSF for 24 h was analyzed by qPCR. Expression before RANKL treatment was set at 1. (G) Mature OCs were incubated on whole dentine slices with M-CSF and LPS with or without 3-methyladenine (3-MA, 3 mM) for 3 days. Slices were stained with Mayer's hematoxylin. Representative photos of resorption pits formed by LPS-induced OCs are shown. Scale bar: 50 μm. Resorption pit areas were measured. Results are expressed as means ± SEM of 3-6 cultures per variable. $^{**}P < 0.01$; $^{***}P < 0.001$ compared with vehicle (V)-treated cells. $^{\#}P < 0.05$; $^{\#\#}P < 0.01$~ compared with LPS-treated cells. Similar results were obtained in three independent experiments.

RESULTS

LPS stimulates OC formation in RANKL-treated pre-OCs *in vitro*

To investigate a direct effect of LPS on pre-OCs, we examined whether LPS increased OC formation and bone resorption, in conditions that excluded the effects of other cells. Since LPS inhibited OC differentiation when given simultaneously with RANKL as previously reported (Takami et al., 2002), RANKL-treated OC precursor cells were stimulated with LPS to drive the cells to differentiate into OCs. Exposure to LPS for 48 h resulted in maximal OC formation as shown by counting TRAP-positive MNCs (Figs. 1A-1E), The number, the maximum diameter, and the area of OCs formed in response to LPS stimulation was reduced compared to those formed in response to RANKL without LPS (Figs. 1A-1D). Furthermore, the fusion index which was expressed as the mean number of nuclei per TRAP-positive MNC induced by LPS was also lower than that by RANKL (Fig. 1E). Consistent with increased OC formation, transcripts of TRAP, cathepsin K, calcitonin receptor, DC-STAMP, and ATP6v0d2 were higher in LPS-treated cells than in vehicle-treated cells (Fig. 1F). Next, we examined whether LPS also elevated bone resorption *in vitro*. Mature OCs formed substantial numbers of pits on dentine slices after LPS treatment. LPS increased the overall area of pits, compared with vehicle-treated cells (Fig. 1G), suggesting that LPS enhances the activity of OCs.

LPS stimulates OC formation by inducing autophagy

Autophagy has been reported to increase the number and function of OCs (DeSelm et al., 2011; Xiu et al., 2014). Inflammation, represented by elevated TNF-α, induces bone destruction in rheumatoid arthritis via enhanced autophagy (Cejka et al., 2010). Based on these, we hypothesized that LPS increases the formation of OCs by inducing autophagy. We evaluated LPS-induced autophagy by two methods (Chen et al., 2010; Sharifi et al., 2015). Autophagosome formation was detected by immunoblotting cell lysates with an antibody against microtubule-associated protein light chain 3 (LC3). As shown in Fig. 2A, LPS increased the lipidated form of LC3 (LC3II), which is the most straightforward indicator of autophagic flux (Sharifi et al., 2015). Since LC3II

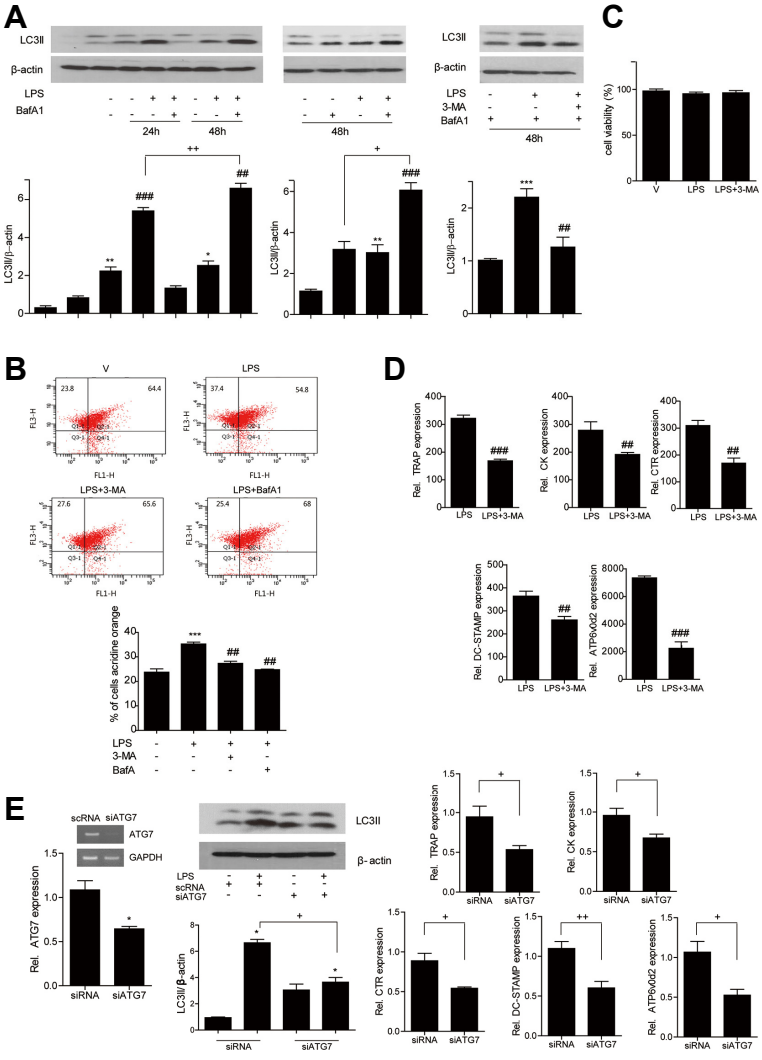

Fig. 2. LPS induces autophagy, increasing OC formation. BMMs were prepared and incubated with M-CSF (M, 30 ng/ml) and RANKL (R, 40 ng/ml) for 40 h, washed thoroughly, and incubated further with LPS (50 ng/ml) and M-CSF under the indicated conditions. (A) Formation of LC3II after stimulation with LPS and the indicated treatments. Bafilomycin A1 (30 ng/ml) was added 4 h before harvest to induce accumulation of LC3II, as indicated. Quantification of LC3II normalized to β-actin was plotted. (B) LPS-induced AVO formation was analyzed by flow cytometry. FL-1H indicated green color intensity (cytoplasm and nucleus), while FL3-H showed red color intensity (AVO). As a positive control, LPS was added with bafilomycin A1. (C) Cell viability was measured by MTT assay. Pre OCs treated with LPS were incubated with or without 3-MA (3 mM). After 48 h, cells were washed and incubated with MTT (3-(4,5-Dimethylthiazol-2-yl)-2,5-Diphenyltetrazolium Bromide) for 3 h and lysed in 50% dimethylformamide. Absorbance was determined at 595 nm with a microplate reader. (D) RNA from cells stimulated with LPS with or without 3-MA (3 mM) for 24 h was analyzed by qPCR. (E) BMMs were incubated with M-CSF and RANKL for 40 h, washed completely, transfected with scRNA or siATG7, and incubated further for the indicated periods with LPS and M-CSF. Down-regulation of ATG7 by siRNA was confirmed by RT-PCR and qPCR. RNA for OC-specific genes (24 h) and formation of LC3II (48 h) were analyzed. $*P < 0.05$; $**P < 0.01$; $***P < 0.001$ compared with vehicle (V)-treated cells. $\#\#P < 0.01$; $\#\#\#P < 0.001$ compared with LPS-treated cells. $^{+}P < 0.05$; $^{++}P < 0.01$ between the indicated 2 groups. Similar results were obtained in three independent experiments.

is continuously degraded in autophagolysosomes during autophagy, addition of bafilomycin A1 is recommended to demonstrate autophagic flux (Sharifi et al., 2015). Addition of bafilomycin A1 in LPS-treated OC resulted in a more pronounced increase of LC3II than vehicle-treatment. We also evaluated LPS-induced autophagy by determining the formation of acidic vesicular organelles (AVOs, which include autolysosomes) by flow cytometry using the pH-sensitive fluorescent dye acridine orange. As shown in Fig. 2B, increased levels of LPS-induced AVOs were observed but only at 48 h, whereas elevated levels of LPS-induced LC3II were observed after 24 h (Fig. 2A), supporting the idea that formation of autophagosomes precedes that of autolysosomes. To confirm that LPS induces autophagy in pre-OCs, 3-methyladenine (3-MA) was added, as an autophagy inhibitor, and significantly decreased LPS-induced LC3 II formation in the presence of bafilomycin A (Fig. 2A). The formation of LPS-induced AVOs was also inhibited by 3-MA: the percentage of cells with AVOs was reduced from 37.4% to 27.6% by 3-MA (Fig. 2B). Similar pattern was observed with treatment of bafilomycin A1. 3-MA did not have any detrimental effect on the viability of OC under the assayed conditions (Fig. 2C). Next, we determined the effect of inhibition of autophagy on OC-specific gene expression. As shown in Fig. 2D, 3-MA opposed the LPS-stimulated increases in transcripts of TRAP, cathepsin K, calcitonin receptor, DC-STAMP, and ATP6v0d2. In addition, 3-MA significantly decreased the areas of pits induced by LPS (Fig. 1G). To confirm that the effect of LPS on OC was due to LPS-induced autophagy, we examined the effect of ATG7 silencing. Knockdown of ATG7 attenuated LPS-induced LC3II level as well as LPS-induced OC-specific genes (Fig. 2E).

LPS promotes autophagy leading to OC formation by stimulating ROS production

RANKL induces a sustaining increase of cytoplasmic ROS, leading to OC differentiation (Lee et al., 2005) and ROS induce autophagy (Chen et al., 2009). We examined whether LPS increased cytoplasmic ROS level in pre-OCs primed by RANKL. LPS indeed elevated ROS to a maximum level after 24 h (Fig. 3A). The ROS scavenger, N-acetylcysteine (NAC), decreased LPS-induced ROS level and OC-specific gene expression (Figs. 3A and 3B). As expected, it also decreased autophagy flux activity in response to LPS (Fig. 3C), demonstrating that LPS-induced autophagy is mediated by ROS. To determine the effect of ROS production on LPS-induced autophagy, we manipulated the cellular levels of ROS by reducing the level of NOX1 or/and NOX2 by siRNA knockdown (Fig. 4A). Both siNOX2 and siNOX1 reduced LPS-stimulated OC-specific genes expression as well as cytoplasmic ROS to a modest degree, whereas the combination of siNOX1 and siNOX2 was more effective for reducing those (Figs. 4B and 4C). Moreover LPS-induced LC3II accumulation was dramatically decreased by the combination of siNOX1 and siNOX2 (Fig. 4D). These results indicated that LPS-induced ROS enhanced autophagy in pre-OCs. Next, we wondered whether autophagy might also affect the accumulation of ROS. However, blockade of autophagy by 3-MA

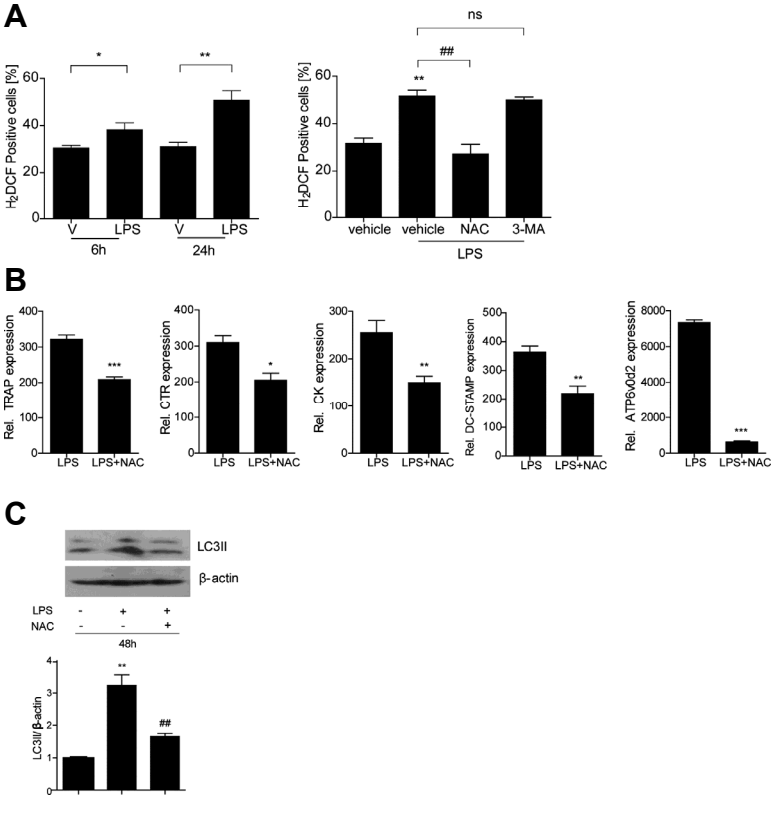

Fig. 3. LPS promotes the accumulation of ROS, which leads to autophagy. (A-C) BMMs were prepared and incubated with M-CSF (M, 30ng/ml) and RANKL (R, 40 ng/ml) for 40 h, washed thoroughly, and incubated further for the indicated periods with LPS (50 ng/ml) with or without NAC (10 mM) or 3-MA (3 mM). Intracellular ROS after LPS stimulation for 6 h and 24 h was determined by flow cytometry using H_2DCF-DA (A). OC-specific transcripts (B) and formation of LC3II (C) were analyzed after 24 h and 48 h of LPS stimulation, respectively. $*P < 0.05$; $**P < 0.01$ compared with vehicle (V)-treated cells. $\#\#P < 0.01$ compared with LPS-treated cells. Quantification of LC3II normalized to β-actin was plotted.

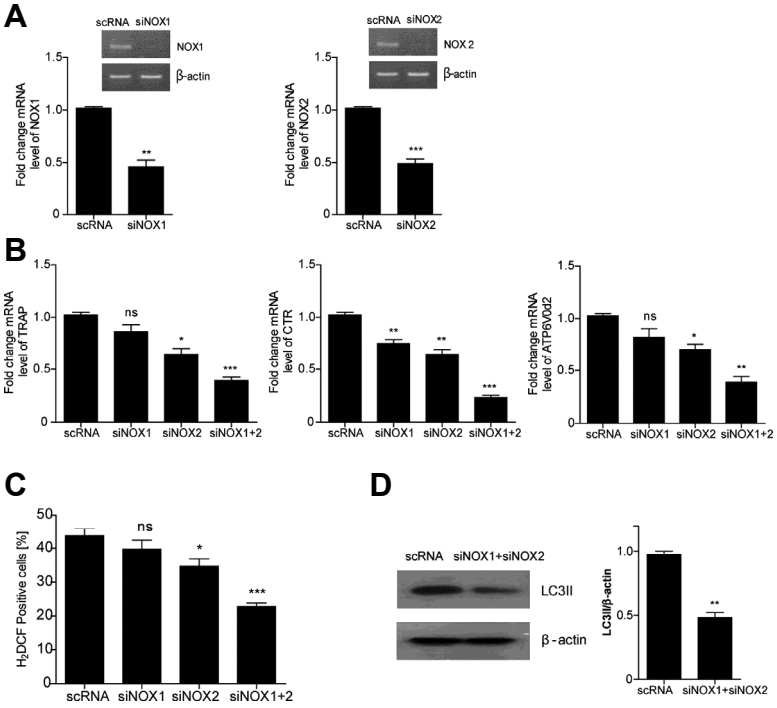

Fig. 4. LPS-induced autophagy is dependent upon ROS formation. BMMs were incubated with M-CSF (M, 30ng/ml) and RANKL (R, 40 ng/ml) for 40 h, washed completely, transfected with scRNA, si-NOX1, siNOX2 or siNOX1+siNOX2, and incubated further for the indicated periods with LPS and M-CSF. Downregulation of NOX1 and NOX2 by siRNA was confirmed by RT-PCR and qPCR (A). Intracellular ROS (24 h) (B), RNA for OC-specific genes (24 h) (C), and formation of LC3II (48 h) (D) were analyzed. $*P < 0.05$; $**P < 0.01$; $***P < 0.001$ compared with scRNA-transfected cells. Similar results were obtained in three independent experiments.

did not alter levels of ROS formed in response to LPS (Fig. 3A), suggesting that ROS act upstream of the Class III PI3K in the process of autophagy in OCs.

DISCUSSION

We have demonstrated that LPS induces OC autophagy as well as osteoclastogenesis *in vitro*. When LPS was applied to RANKL-treated pre-OCs, numbers of OC were increased, as defined by counting TRAP-positive MNCs. TLR stimulation of OC progenitors inhibits their differentiation into mature OC, but maintains phagocytic function (Takami et al., 2002), suggesting that the effect of LPS on OC progenitors is due to response in macrophages, but not in OC. LPS also increased pit areas in dentine slices, thus revealing enhanced OC activity. In addition, LPS elevated transcripts of OC-specific genes including TRAP, calcitonin receptor, cathepsin K, ATP6v0d2 and DC-STAMP. LPS-stimulated OCs exhibited autophagic flux activity evaluated by LC3II accumulation, an authentic marker for autophagy flux activity, and AVO formation, which is indicative of autolysosome formation. Blockage of autophagy with 3-MA decreased LPS-induced OC-specific gene transcripts as well as autophagic flux activity and AVO formation. Silencing of ATG7 also attenuated LPS-induced OC-specific genes as well as LPS-induced LC3II level. These results showed that LPS induced autophagy that plays a critical role in the formation and activity of OCs, suggesting that inhibition of autophagy is a potential treatment for preventing inflammatory bone loss. Several other studies have demonstrated a role of autophagy in OCs. Thus, hypoxia increases OC differentiation as well as autophagic flux as a result of expression of Bcl2/adenovirus E1B 19 kDa interacting protein 3 (Zhao et al., 2012). Mutations affecting the autophagic cargo receptor SQSTM1 (p62) result in Pagetic disorders of the bone in which OCs increase in number and activity (Chamoux et al., 2009). Important roles of autophagy-related proteins associated with autophagosome formation in OCs such as Atg5, Atg7, Atg4B and LC3 have been demonstrated (Chung et al., 2012; DeSelm et al., 2011). Myeloid specific Atg5-deficiency had no effect on OC formation, but impaired OC activity and led to dysfunctional ruffled borders and shallower resorption pits with increased bone volume and reduced OVX-induced bone loss *in vivo* (DeSelm et al., 2011). Myeloid specific deletion of Atg7 had similar results (DeSelm et al., 2011), implying that autophagy plays a critical role in ruffled border formation and so is indispensible for bone resorption. These findings are supported by the observation that LC3 deficiency leads to impaired actin ring formation and resorption (Chung et al., 2012). In addition, hematopoietic stem cells fail to differentiate, and genomic and cellular damage accumulates in the absence of Atg7 (Wang et al., 2011), implying that autophagy is important for generating hematopoietic stem cells, the pool of OC precursors. These studies showed that autophagy plays a role in regulating the precursor pool, differentiation, and activity of OCs, although the detailed mechanisms and interactions with other cells are not clear.

In our studies, LPS induced a sustained level of cytoplasmic ROS along with elevated differentiation to OCs. Decreasing ROS with the antioxidant, NAC, or combined knockdowns of NOX1 and NOX2, decreased both the formation of OCs and autophagy in response to LPS, demonstrating that ROS are associated with LPS-induced differentiation as well as autophagy. This view is supported by the finding that oxida-

tive stress induced autophagy and OC differentiation (Wang et al., 2011). The participation of ROS in autophagic processes has been demonstrated in several other systems. Thus, starvation increased ROS as well as autophagy (Shi et al., 2015). Administration of NAC reduced the induction of autophagy by lowering ROS in neurons (Scherz-Shouval et al., 2007), whereas stimulation of NOX promoted autophagy in phagosomes (Kirkland et al., 2002). ROS are involved directly in thiol modification of Cys residues in ATG4 during starvation-induced autophagy (Shi et al., 2015) and indirectly through Nrf2 by increasing the level of the autophagic proteins p62 (Huang and Brumell, 2009) and p53 and so increasing sestrin (Fujita et al., 2011). Since oxidation of mTOR reduces its activity (Budanov and Karin, 2008), mTOR may be a target of ROS. The activity of the beclin-1-class III PI3K complex may also be a target due to the redox-sensitive cysteine-rich domains of autophagy factor-1 (Dames et al., 2005) and Rubicon (Chang et al., 2010), which suggests that redox regulation may play a key role in the process of autophagy. However, we showed that 3-MA did not decrease LPS-induced ROS in OCs, suggesting that ROS lie upstream of the class III PI3K in the process of autophagy. Similar findings have been reported by others: 3-MA did not decrease ROS levels in starvation-induced autophagy (Chen et al., 2009) or in dexamethasone-induced autophagy (Zhong et al., 2009).

In conclusion, our studies show that LPS stimulates OC differentiation from pre-OCs by enhancing autophagy as a result of raising ROS levels in pre-OCs. The present findings suggest that autophagy and ROS levels might be targeted therapeutically to reduce inflammatory bone loss.

ACKNOWLEDGMENTS

This work was supported by the Basic Science Research Program (2015R1A2A2A01002417) of NRF funded by the Korean government. OJS (2016R1A6A3A11932375) and HJP (2014R1A6A1030318) were supported by the BSRP of the NRF, and the NRF fund through the Ministry of Education, respectively.

REFERENCES

Budanov, A.V., and Karin, M. (2008). p53 target genes sestrin1 and sestrin2 connect genotoxic stress and mTOR signaling. Cell *134*, 451-460.

Cejka, D., Hayer, S., Niederreiter, B., Sieghart, W., Fuereder, T., Zwerina, J., and Schett, G. (2010). Mammalian target of rapamycin signaling is crucial for joint destruction in experimental arthritis and is activated in osteoclasts from patients with rheumatoid arthritis. Arthritis Rheum. *62*, 2294-2302.

Chamoux, E., Couture, J., Bisson, M., Morissette, J., Brown, J.P., and Roux, S. (2009). The p62 P392L mutation linked to Paget's disease induces activation of human osteoclasts. Mol. Endocrinol. *23*, 1668-1680.

Chang, N.C., Nguyen, M., Germain, M., and Shore, G.C. (2010). Antagonism of Beclin 1-dependent autophagy by BCL-2 at the endoplasmic reticulum requires NAF-1. EMBO J. *29*, 606-618.

Chen, Y., McMillan-Ward, E., Kong, J., Israels, S.J., and Gibson, S.B. (2007). Mitochondrial electron-transport-chain inhibitors of complexes I and II induce autophagic cell death mediated by reactive oxygen species. J. Cell Sci. *120*, 4155-4166.

Chen, Y., Azad, M.B., and Gibson, S.B. (2009). Superoxide is the major reactive oxygen species regulating autophagy. Cell Death Differ. *16*, 1040-1052.

Chung, Y.H., Yoon, S.Y., Choi, B., Sohn, D.H., Yoon, K.H., Kim, W.J., Kim, D.H., and Chang, E.J. (2012). Microtubule-associated protein light chain 3 regulates Cdc42-dependent actin ring formation in osteoclast. Int. J. Biochem. Cell Biol. *44*, 989-997.

Dames, S.A., Mulet, J.M., Rathgeb-Szabo, K., Hall, M.N., and Grzesiek, S. (2005). The solution structure of the FATC domain of the protein kinase target of rapamycin suggests a role for redox-dependent structural and cellular stability. J. Biol. Chem. *280*, 20558-20564.

DeSelm, C.J., Miller, B.C., Zou, W., Beatty, W.L., van Meel, E., Takahata, Y., Klumperman, J., Tooze, S.A., Teitelbaum, S.L., and Virgin, H.W. (2011). Autophagy proteins regulate the secretory component of osteoclastic bone resorption. Dev. Cell *21*, 966-974.

Fujita, K., Maeda, D., Xiao, Q., and Srinivasula, S.M. (2011). Nrf2-mediated induction of p62 controls Toll-like receptor-4-driven aggresome-like induced structure formation and autophagic degradation. Proc. Natl. Acad. Sci. USA *108*, 1427-1432.

Huang, J., and Brumell, J.H. (2009). NADPH oxidases contribute to autophagy regulation. Autophagy *5*, 887-889.

Jimi, E., Akiyama, S., Tsuruka,i T., Okahashi, N., Kobayashi, K., Udagawa, N., Nishihara, T., and Suda, T. (1999). Osteoclast differentiation factor acts as a multifunctional regulator in murine osteoclast differentiation and function. J. Immunol. *163*, 434-442.

Ke, K., Sul, O.J., Choi, E.K., Safdar, A.M., Kim, E.S., and Choi, H.S. (2014). Reactive oxygen species induce the association of SHP-1 with c-Src and the oxidation of both to enhance osteoclast survival. Am. J. Physiol. Endocrinol. Metab. *307*, E61-E70

Kirkland, R.A., Adibhatla, R.M., Hatcher, J.F., and Franklin, J.L. (2002). Loss of cardiolipin and mitochondria during programmed neuronal death: evidence of a role for lipid peroxidation and autophagy. Neuroscience *115*, 587-602.

Lee, N.K., Choi, Y.G., Baik, J.Y., Han, S.Y., Jeong, D.W., Bae, Y.S., Kim, N., and Lee, S.Y. (2005). A crucial role for reactive oxygen species in RANKL-induced osteoclast differentiation. Blood *106*, 852-859.

Lin, N.Y., Beyer, C., Giessl, A., Kireva, T., Scholtysek, C., Uderhardt, S., Munoz, L.E., Dees, C., Distler, A., Wirtz, S., et al. (2013). Autophagy regulates TNFα-mediated joint destruction in experimental arthritis. Ann. Rheum. Dis. *72*, 761-768.

Orcel, P., Feuga, M., Bielakoff, J., and De Vernejoul, M.C. (1993). Local bone injections of LPS and M-CSF increase bone resorption by different pathways in vivo in rats. Am. J. Physiol. *264*, E391-397.

Park, H., Noh, A., Long, S.M., Kang, J., Sim, J., Lee, D., and Yim, M. (2014). Peroxiredoxin II negatively regulates lipopolysaccharide-induced osteoclast formation and bone loss via JNK and STAT3. Antioxid. Redox Signal. *22*, 63-77.

Sato, M., Bryant, H.U., Dodge, J.A., Davis, H., Matter, W.F., and Vlahos, C.J. (1996). Effects of wortmannin analogs on bone *in vitro* and *in vivo*. J. Pharmacol. Exp. Ther. *277*, 543-550.

Scherz-Shouval, R., Shvets, E., Fass, E., Shorer, H., Gil, L., and Elazar, Z. (2007). Reactive oxygen species are essential for autophagy and specifically regulate the activity of Atg4. EMBO J. *26*, 1749-1760.

Sharifi, M.N., Mowers, E.E., Drake, L.E., and Macleod, K.F. (2015). Measuring autophagy in stressed cells. Methods Mol. Biol. *1292*, 129-150.

Shi, J., Wang, L., Zhang, H., Jie, Q., Li, X., Shi, Q., Huang, Q., Gao, B., Han, Y., Guo, K., et al. (2015). Glucocorticoids: dose-related effects

on osteoclast formation and function via reactive oxygen species and autophagy. Bone *79*, 222-232.

Takami, M., Kim, N., Rho, J., and Choi, Y. (2002). Stimulation by toll-like receptors inhibits osteoclast differentiation. J. Immunol. *169*, 1516-1523.

Ti, Y., Zhou, L., Wang, R., and Zhao, J. (2015). Inhibition of microtubule dynamics affects podosome belt formation during osteoclast induction. Cell Biochem. Biophys. *71*, 741-747.

Wang, K., Niu, J., Kim, H., and Kolattukudy, P.E. (2011). Osteoclast precursor differentiation by MCPIP via oxidative stress, endoplasmic reticulum stress, and autophagy. J. Mol. Cell Biol. 3, 360-368.

Xiu, Y., Xu, H., Zhao, C., Li, J., Morita, Y., Yao, Z., Xin, L., and Boyce, B.F. (2014). Chloroquine reduces osteoclastogenesis in murine osteoporosis by preventing TRAF3 degradation. J. Clin. Invest. *124*, 297-310.

Zhang, L., Guo, Y.F., Liu, Y.Z., Liu, Y.J., Xiong, D.H., Liu, X.G., Wang, L., Yang, T.L., Lei, S.F., Guo, Y., et al. (2010). Pathway-based genome-wide association analysis identified the importance of regulation-of-autophagy pathway for ultradistal radius BMD. J. Bone Miner. Res. *25*, 1572-1580.

Zhao, Y., Chen, G., Zhang, W., Xu, N., Zhu, J.Y., Jia, J., Sun, Z.J., Wang, Y.N., and Zhao, Y.F. (2012). Autophagy regulates hypoxia-induced osteoclastogenesis through the HIF-1α/BNIP3 signaling pathway. J. Cell. Physiol. *227*, 639-648.

Zhong, Y., Wang, Q.J., Li, X., Yan, Y., Backer, J.M., Chait, B.T., Heintz, N., and Yue, Z. (2009). Distinct regulation of autophagic activity by Atg14L and Rubicon associated with Beclin 1-phosphatidylinositol-3-kinase complex. Nat. Cell Biol. *11*, 468-476.